



Search for Doubly Charged Higgs Bosons at LEP2

J. Abdallah, P. Abreu, W. Adam, P. Adzic, T. Albrecht, T. Alderweireld, R. Alemany-Fernandez, T. Allmendinger, P P. Allport, U. Amaldi, et al.

► To cite this version:

J. Abdallah, P. Abreu, W. Adam, P. Adzic, T. Albrecht, et al.. Search for Doubly Charged Higgs Bosons at LEP2. Physics Letters B, 2003, 552, pp.127-137. 10.1016/S0370-2693(02)03125-8 . in2p3-00012366

HAL Id: in2p3-00012366

<https://hal.in2p3.fr/in2p3-00012366>

Submitted on 8 Jan 2003

HAL is a multi-disciplinary open access archive for the deposit and dissemination of scientific research documents, whether they are published or not. The documents may come from teaching and research institutions in France or abroad, or from public or private research centers.

L'archive ouverte pluridisciplinaire **HAL**, est destinée au dépôt et à la diffusion de documents scientifiques de niveau recherche, publiés ou non, émanant des établissements d'enseignement et de recherche français ou étrangers, des laboratoires publics ou privés.

Search for Doubly Charged Higgs Bosons at LEP2

DELPHI Collaboration

Abstract

A search for pair-produced doubly charged Higgs bosons has been performed using the data collected by the DELPHI detector at LEP at centre-of-mass energies between 189 and 209 GeV. No excess is observed in the data with respect to the Standard Model background. A lower limit for the mass of 97.3 GeV/ c^2 at the 95% confidence level has been set for doubly charged Higgs bosons in left-right symmetric models for any value of the Yukawa coupling between the Higgs bosons and the τ leptons.

This paper is dedicated to the memory of Paolo Poropat.

(Submitted to Phys. Lett. B)

J.Abdallah²⁴, P.Abreu²², W.Adam⁵⁰, P.Adzic¹¹, T.Albrecht¹⁷, T.Alderweireld², R.Aleman-Fernandez⁸, T.Allmendinger¹⁷, P.P.Allport²³, U.Amaldi²⁸, N.Amapane⁴⁴, S.Amato⁴⁷, E.Anashkin³⁵, A.Andreazza²⁷, S.Andringa²², N.Anjos²², P.Antilogus²⁶, W-D.Apel¹⁷, Y.Arnoud¹⁴, S.Ask²⁵, B.Asman⁴³, J.E.Augustin²⁴, A.Augustinus⁸, P.Baillon⁸, A.Ballestrero⁴⁵, P.Bambade²⁰, R.Barbier²⁶, D.Bardin¹⁶, G.Barker¹⁷, A.Baroncelli³⁸, M.Battaglia⁸, M.Baubillier²⁴, K-H.Becks⁵², M.Begalli⁶, A.Behrmann⁵², E.Ben-Haim²⁰, N.Benekos³¹, A.Benvenuti⁵, C.Berat¹⁴, M.Berggren²⁴, L.Berntzon⁴³, D.Bertrand², M.Besancon³⁹, N.Besson³⁹, D.Bloch⁹, M.Blom³⁰, M.Bluj⁵¹, M.Bonesini²⁸, M.Boonekamp³⁹, P.S.L.Booth²³, G.Borisov²¹, O.Botner⁴⁸, B.Bouquet²⁰, T.J.V.Bowcock²³, I.Boyko¹⁶, M.Bracko⁴², R.Brenner⁴⁸, E.Brodet³⁴, P.Bruckman¹⁸, J.M.Brunet⁷, L.Bugge³², P.Buschmann⁵², M.Calvi²⁸, T.Camporesi⁸, V.Canale³⁷, F.Carena⁸, N.Castro²², F.Cavallo⁵, M.Chapkin⁴¹, Ph.Charpentier⁸, P.Checchia³⁵, R.Chierici⁸, P.Chliapnikov⁴¹, J.Chudoba⁸, S.U.Chung⁸, K.Cieslik¹⁸, P.Collins⁸, R.Contri¹³, G.Cosme²⁰, F.Cossutti⁴⁶, M.J.Costa⁴⁹, B.Crawley¹, D.Crennell³⁶, J.Cuevas³³, J.D'Hondt², J.Dalmau⁴³, T.da Silva⁴⁷, W.Da Silva²⁴, G.Della Ricca⁴⁶, A.De Angelis⁴⁶, W.De Boer¹⁷, C.De Clercq², B.De Lotto⁴⁶, N.De Maria⁴⁴, A.De Min³⁵, L.de Paula⁴⁷, L.Di Ciaccio³⁷, A.Di Simone³⁸, K.Doroba⁵¹, J.Drees^{52,8}, M.Dris³¹, G.Eigen⁴, T.Ekelof⁴⁸, M.Ellert⁴⁸, M.Elsing⁸, M.C.Espirito Santo⁸, G.Fanourakis¹¹, D.Fassouliotis^{11,3}, M.Feindt¹⁷, J.Fernandez⁴⁰, A.Ferrer⁴⁹, F.Ferro¹³, U.Flagmeyer⁵², H.Foeth⁸, E.Fokitis³¹, F.Fulda-Quenzer²⁰, J.Fuster⁴⁹, M.Gandelman⁴⁷, C.Garcia⁴⁹, Ph.Gavillet⁸, E.Gazis³¹, T.Geralis¹¹, R.Gokieli^{8,51}, B.Golob⁴², G.Gomez-Ceballos⁴⁰, P.Goncalves²², E.Graziani³⁸, G.Grosdidier²⁰, K.Grzelak⁵¹, J.Guy³⁶, C.Haag¹⁷, A.Hallgren⁴⁸, K.Hamacher⁵², K.Hamilton³⁴, J.Hansen³², S.Haug³², F.Hauler¹⁷, V.Hedberg²⁵, M.Hennecke¹⁷, H.Herr⁸, J.Hoffman⁵¹, S-O.Holmgren⁴³, P.J.Holt⁸, M.A.Houlden²³, K.Hultqvist⁴³, J.N.Jackson²³, G.Jarlskog²⁵, P.Jarry³⁹, D.Jeans³⁴, E.K.Johansson⁴³, P.D.Johansson⁴³, P.Jonsson²⁶, C.Joram³⁵, L.Jungermann¹⁷, F.Kapusta²⁴, S.Katsanevas²⁶, E.Katsoufis³¹, G.Kernel⁴², B.P.Kersevan^{8,42}, A.Kiiskinen¹⁵, B.T.King²³, N.J.Kjaer⁸, P.Kluit³⁰, P.Kokkinias¹¹, C.Kourkoumelis³, O.Kouznetsov¹⁶, Z.Krumstein¹⁶, M.Kucharczyk¹⁸, J.Lamsa¹, G.Leder⁵⁰, F.Ledroit¹⁴, L.Leinonen⁴³, R.Leitner²⁹, J.Lemonne², V.Lepeltier²⁰, T.Lesiak¹⁸, W.Liebig⁵², D.Liko⁵⁰, A.Lipniacka⁴³, J.H.Lopes⁴⁷, J.M.Lopez³³, D.Loukas¹¹, P.Lutz³⁹, L.Lyons³⁴, J.MacNaughton⁵⁰, A.Malek⁵², S.Maltezos³¹, F.Mandl⁵⁰, J.Marco⁴⁰, R.Marco⁴⁰, B.Marechal⁴⁷, M.Margoni³⁵, J-C.Marin⁸, C.Mariotti⁸, A.Markou¹¹, C.Martinez-Rivero⁴⁰, J.Masik¹², N.Mastroiannopoulos¹¹, F.Matorras⁴⁰, C.Matteuzzi²⁸, F.Mazzucato³⁵, M.Mazzucato³⁵, R.Mc Nulty²³, C.Meroni²⁷, W.T.Meyer¹, E.Migliore⁴⁴, W.Mitaroff⁵⁰, U.Mjoernmark²⁵, T.Moa⁴³, M.Moch¹⁷, K.Moenig^{8,10}, R.Monge¹³, J.Montenegro³⁰, D.Moraes⁴⁷, S.Moreno²², P.Moretini¹³, U.Mueller⁵², K.Muenich⁵², M.Mulders³⁰, L.Mundim⁶, W.Murray³⁶, B.Muryn¹⁹, G.Myatt³⁴, T.Myklebust³², M.Nassiakou¹¹, F.Navarria⁵, K.Nawrocki⁵¹, R.Nicolaidou³⁹, M.Nikolenko^{16,9}, A.Oblakowska-Mucha¹⁹, V.Obratsov⁴¹, A.Olshevski¹⁶, A.Onofre²², R.Orava¹⁵, K.Osterberg¹⁵, A.Ouraou³⁹, A.Oyanguren⁴⁹, M.Paganoni²⁸, S.Paiano⁵, J.P.Palacios²³, H.Palka¹⁸, Th.D.Papadopoulou³¹, L.Pape⁸, C.Parkes²³, F.Parodi¹³, U.Parzefall⁸, A.Passeri³⁸, O.Passon⁵², L.Peralta²², V.Perepelitsa⁴⁹, A.Perrotta⁵, A.Petrolini¹³, J.Piedra⁴⁰, L.Pieri³⁸, F.Pierre³⁹, M.Pimenta²², E.Piotto⁸, T.Podobnik⁴², V.Poireau³⁹, M.E.Pol⁶, G.Polok¹⁸, P.Poropat⁴⁶, V.Pozdniakov¹⁶, N.Pukhaeva^{2,16}, A.Pullia²⁸, J.Rames¹², L.Ramler¹⁷, A.Read³², P.Rebecchi⁸, J.Rehn¹⁷, D.Reid³⁰, R.Reinhardt⁵², P.Renton³⁴, F.Richard²⁰, J.Ridky¹², M.Rivero⁴⁰, D.Rodriguez⁴⁰, A.Romero⁴⁴, P.Ronchese³⁵, E.Rosenberg¹, P.Roudeau²⁰, T.Rovelli⁵, V.Ruhmann-Kleider³⁹, D.Ryabtchikov⁴¹, A.Sadovsky¹⁶, L.Salmi¹⁵, J.Salt⁴⁹, A.Savoy-Navarro²⁴, U.Schwickerath⁸, A.Segar³⁴, R.Sekulin³⁶, M.Siebel⁵², A.Sisakian¹⁶, G.Smadja²⁶, O.Smirnova²⁵, A.Sokolov⁴¹, A.Sopczak²¹, R.Sosnowski⁵¹, T.Spaso⁸, M.Stanitzki¹⁷, A.Stocchi²⁰, J.Strauss⁵⁰, B.Stugu⁴, M.Szczekowski⁵¹, M.Szeptycka⁵¹, T.Szumlak¹⁹, T.Tabarelli²⁸, A.C.Taffard²³, F.Tegenfeldt⁴⁸, J.Timmermans³⁰, L.Tkatchev¹⁶, M.Tobin²³, S.Todorovova¹², A.Tomaradze⁸, B.Tome²², A.Tonazzo²⁸, P.Tortosa⁴⁹, P.Travnicek¹², D.Treille⁸, G.Tristram⁷, M.Trochimczuk⁵¹, C.Troncon²⁷, M-L.Turluer³⁹, I.A.Tyapkin¹⁶, P.Tyapkin¹⁶, S.Tzamarias¹¹, V.Uvarov⁴¹, G.Valenti⁵, P.Van Dam³⁰, J.Van Eldik⁸, A.Van Lysebetten², N.van Remortel², I.Van Vulpen³⁰, G.Vegni²⁷, F.Veloso²², W.Venus³⁶, F.Verbeure², P.Verdier²⁶, V.Verzi³⁷, D.Vilanova³⁹, L.Vitale⁴⁶, V.Vrba¹², H.Wahlen⁵²,

A.J.Washbrook²³, C.Weiser¹⁷, D.Wicke⁸, J.Wickens², G.Wilkinson³⁴, M.Winter⁹, M.Witek¹⁸, O.Yushchenko⁴¹,
A.Zalewska¹⁸, P.Zalewski⁵¹, D.Zavrtanik⁴², N.I.Zimin¹⁶, A.Zintchenko¹⁶, M.Zupan¹¹

-
- ¹Department of Physics and Astronomy, Iowa State University, Ames IA 50011-3160, USA
²Physics Department, Universiteit Antwerpen, Universiteitsplein 1, B-2610 Antwerpen, Belgium
and IIHE, ULB-VUB, Pleinlaan 2, B-1050 Brussels, Belgium
and Faculté des Sciences, Univ. de l'Etat Mons, Av. Maistriau 19, B-7000 Mons, Belgium
³Physics Laboratory, University of Athens, Solonos Str. 104, GR-10680 Athens, Greece
⁴Department of Physics, University of Bergen, Allégaten 55, NO-5007 Bergen, Norway
⁵Dipartimento di Fisica, Università di Bologna and INFN, Via Irnerio 46, IT-40126 Bologna, Italy
⁶Centro Brasileiro de Pesquisas Físicas, rua Xavier Sigaud 150, BR-22290 Rio de Janeiro, Brazil
and Depto. de Física, Pont. Univ. Católica, C.P. 38071 BR-22453 Rio de Janeiro, Brazil
and Inst. de Física, Univ. Estadual do Rio de Janeiro, rua São Francisco Xavier 524, Rio de Janeiro, Brazil
⁷Collège de France, Lab. de Physique Corpusculaire, IN2P3-CNRS, FR-75231 Paris Cedex 05, France
⁸CERN, CH-1211 Geneva 23, Switzerland
⁹Institut de Recherches Subatomiques, IN2P3 - CNRS/ULP - BP20, FR-67037 Strasbourg Cedex, France
¹⁰Now at DESY-Zeuthen, Platanenallee 6, D-15735 Zeuthen, Germany
¹¹Institute of Nuclear Physics, N.C.S.R. Demokritos, P.O. Box 60228, GR-15310 Athens, Greece
¹²FZU, Inst. of Phys. of the C.A.S. High Energy Physics Division, Na Slovance 2, CZ-180 40, Praha 8, Czech Republic
¹³Dipartimento di Fisica, Università di Genova and INFN, Via Dodecaneso 33, IT-16146 Genova, Italy
¹⁴Institut des Sciences Nucléaires, IN2P3-CNRS, Université de Grenoble 1, FR-38026 Grenoble Cedex, France
¹⁵Helsinki Institute of Physics, HIP, P.O. Box 9, FI-00014 Helsinki, Finland
¹⁶Joint Institute for Nuclear Research, Dubna, Head Post Office, P.O. Box 79, RU-101 000 Moscow, Russian Federation
¹⁷Institut für Experimentelle Kernphysik, Universität Karlsruhe, Postfach 6980, DE-76128 Karlsruhe, Germany
¹⁸Institute of Nuclear Physics, Ul. Kawary 26a, PL-30055 Krakow, Poland
¹⁹Faculty of Physics and Nuclear Techniques, University of Mining and Metallurgy, PL-30055 Krakow, Poland
²⁰Université de Paris-Sud, Lab. de l'Accélérateur Linéaire, IN2P3-CNRS, Bât. 200, FR-91405 Orsay Cedex, France
²¹School of Physics and Chemistry, University of Lancaster, Lancaster LA1 4YB, UK
²²LIP, IST, FCUL - Av. Elias Garcia, 14-1º, PT-1000 Lisboa Codex, Portugal
²³Department of Physics, University of Liverpool, P.O. Box 147, Liverpool L69 3BX, UK
²⁴LPNHE, IN2P3-CNRS, Univ. Paris VI et VII, Tour 33 (RdC), 4 place Jussieu, FR-75252 Paris Cedex 05, France
²⁵Department of Physics, University of Lund, Sölvegatan 14, SE-223 63 Lund, Sweden
²⁶Université Claude Bernard de Lyon, IPNL, IN2P3-CNRS, FR-69622 Villeurbanne Cedex, France
²⁷Dipartimento di Fisica, Università di Milano and INFN-MILANO, Via Celoria 16, IT-20133 Milan, Italy
²⁸Dipartimento di Fisica, Univ. di Milano-Bicocca and INFN-MILANO, Piazza della Scienza 2, IT-20126 Milan, Italy
²⁹IPNP of MFF, Charles Univ., Areal MFF, V Holesovickach 2, CZ-180 00, Praha 8, Czech Republic
³⁰NIKHEF, Postbus 41882, NL-1009 DB Amsterdam, The Netherlands
³¹National Technical University, Physics Department, Zografou Campus, GR-15773 Athens, Greece
³²Physics Department, University of Oslo, Blindern, NO-0316 Oslo, Norway
³³Dpto. Física, Univ. Oviedo, Avda. Calvo Sotelo s/n, ES-33007 Oviedo, Spain
³⁴Department of Physics, University of Oxford, Keble Road, Oxford OX1 3RH, UK
³⁵Dipartimento di Fisica, Università di Padova and INFN, Via Marzolo 8, IT-35131 Padua, Italy
³⁶Rutherford Appleton Laboratory, Chilton, Didcot OX11 0QX, UK
³⁷Dipartimento di Fisica, Università di Roma II and INFN, Tor Vergata, IT-00173 Rome, Italy
³⁸Dipartimento di Fisica, Università di Roma III and INFN, Via della Vasca Navale 84, IT-00146 Rome, Italy
³⁹DAPNIA/Service de Physique des Particules, CEA-Saclay, FR-91191 Gif-sur-Yvette Cedex, France
⁴⁰Instituto de Física de Cantabria (CSIC-UC), Avda. los Castros s/n, ES-39006 Santander, Spain
⁴¹Inst. for High Energy Physics, Serpukov P.O. Box 35, Protvino, (Moscow Region), Russian Federation
⁴²J. Stefan Institute, Jamova 39, SI-1000 Ljubljana, Slovenia and Laboratory for Astroparticle Physics,
Nova Gorica Polytechnic, Kostanjevska 16a, SI-5000 Nova Gorica, Slovenia,
and Department of Physics, University of Ljubljana, SI-1000 Ljubljana, Slovenia
⁴³Fysikum, Stockholm University, Box 6730, SE-113 85 Stockholm, Sweden
⁴⁴Dipartimento di Fisica Sperimentale, Università di Torino and INFN, Via P. Giuria 1, IT-10125 Turin, Italy
⁴⁵INFN, Sezione di Torino, and Dipartimento di Fisica Teorica, Università di Torino, Via P. Giuria 1,
IT-10125 Turin, Italy
⁴⁶Dipartimento di Fisica, Università di Trieste and INFN, Via A. Valerio 2, IT-34127 Trieste, Italy
and Istituto di Fisica, Università di Udine, IT-33100 Udine, Italy
⁴⁷Univ. Federal do Rio de Janeiro, C.P. 68528 Cidade Univ., Ilha do Fundão BR-21945-970 Rio de Janeiro, Brazil
⁴⁸Department of Radiation Sciences, University of Uppsala, P.O. Box 535, SE-751 21 Uppsala, Sweden
⁴⁹IFIC, Valencia-CSIC, and D.F.A.M.N., U. de Valencia, Avda. Dr. Moliner 50, ES-46100 Burjassot (Valencia), Spain
⁵⁰Institut für Hochenergiephysik, Österr. Akad. d. Wissensch., Nikolsdorfergasse 18, AT-1050 Vienna, Austria
⁵¹Inst. Nuclear Studies and University of Warsaw, Ul. Hoza 69, PL-00681 Warsaw, Poland
⁵²Fachbereich Physik, University of Wuppertal, Postfach 100 127, DE-42097 Wuppertal, Germany

† deceased

1 Introduction

Doubly charged Higgs bosons ($H^{\pm\pm}$) appear in several extensions to the Standard Model [1], such as left-right symmetric models, and can be relatively light. In Super-symmetric left-right models usually the $SU(2)_R$ gauge symmetry is broken by two triplet Higgs fields, so-called left and right handed. Pair-production of doubly charged Higgs bosons is expected to occur mainly via s -channel exchange of a photon or a Z boson. In left-right symmetric models the cross-section of $e^+e^- \rightarrow H_L^{++}H_L^{--}$ is different from that for $e^+e^- \rightarrow H_R^{++}H_R^{--}$, where $H_L^{\pm\pm}$ and $H_R^{\pm\pm}$ are the left-handed and right-handed Higgs bosons. The formulae for the decays and the production of these particles can be found in [2].

In these models the doubly charged Higgs boson couples only to charged lepton pairs, other Higgs bosons, and gauge bosons, at the tree level. The current limit and the mass range of this analysis is restricted to the interval between 45 GeV/ c^2 , the LEP1 limit set by OPAL [3], and the kinematic limit at LEP2, that is around 104 GeV/ c^2 . The dominant decay mode of the doubly charged Higgs boson is expected to be a same sign charged lepton pair, the decay proceeding via a lepton number violating coupling. As discussed in [2], due to limits that exist for the couplings of $H^{\pm\pm} \rightarrow e^\pm e^\pm$ from high energy Bhabha scattering, $H^{\pm\pm} \rightarrow \mu^\pm \mu^\pm$ from the absence of muonium to anti-muonium transitions and $H^{\pm\pm} \rightarrow \mu^\pm e^\pm$ from limits on the flavour changing decay $\mu^\pm \rightarrow e^\mp e^\pm e^\pm$, electron and muon decays are not likely. In addition, most of the models expect that the coupling to $\tau\tau$ will be much larger than any of the others. Therefore, only the doubly charged Higgs boson decay $H^{\pm\pm} \rightarrow \tau^\pm \tau^\pm$ is considered here.

The partial width for the $H^{\pm\pm}$ decay into two τ leptons is, at the tree level [2]:

$$\Gamma_{\tau\tau}(H^{\pm\pm} \rightarrow \tau^\pm \tau^\pm) = \frac{h_{\tau\tau}^2}{8\pi} m_H \left(1 - \frac{2m_\tau^2}{m_H^2}\right) \left(1 - \frac{4m_\tau^2}{m_H^2}\right)^{1/2} \quad (1)$$

where m_τ is the mass of the τ lepton and $h_{\tau\tau}$ is the unknown Yukawa coupling constant. Depending on the $h_{\tau\tau}$ coupling and the Higgs boson mass the experimental signature is different. If $h_{\tau\tau}$ is sufficiently large, $h_{\tau\tau} \geq 10^{-7}$, the Higgs boson decays very close to the interaction point. We describe here an analysis to search for such events. If $h_{\tau\tau}$ is smaller the decay occurs inside the tracking detectors or even beyond them, making this analysis inefficient. In this case pre-existing analyses were applied which are further discussed below.

2 Data sample and event generators

The data collected by DELPHI during the LEP runs at centre-of-mass energies from 189 GeV to 209 GeV were used. The total integrated luminosity of these data samples is $\sim 570 \text{ pb}^{-1}$. The DELPHI detector and its performance have already been described in detail elsewhere [4,5].

Signal samples were simulated using the PYTHIA generator [6]. In this analysis samples with doubly charged Higgs boson with masses between 50 and 100 GeV/ c^2 , in 10 GeV/ c^2 steps, were used at different centre-of-mass energies, both for left-handed and right-handed bosons, and different Yukawa coupling constants.

The background estimates from the different Standard Model processes were based on the following event generators, interfaced with the full DELPHI simulation program [5]. The WPHACT [7] generator was used to produce four fermion Monte Carlo simulation

events. The four fermion samples were complemented with dedicated two photon collision samples generated with BDK, BDKRC [8] and PYTHIA [6]. Samples of $q\bar{q}(\gamma)$ and $\mu^+\mu^-(\gamma)$ events were simulated with the KK2f generator [9]. Finally, KORALZ [10] was used to simulate $\tau^+\tau^-(\gamma)$ events and the generator BHWIDE [11] was used for $e^+e^-(\gamma)$ events.

3 Data selection

The search for pair-produced doubly charged Higgs bosons makes use of three different analyses depending on the $h_{\tau\tau}$ coupling or, equivalently, on the mean decay length of the Higgs bosons. When the mean decay length of the Higgs boson is very small, the resulting final state consists of four narrow and low multiplicity jets coming from the interaction point. This analysis is explained in detail in section 3.1. For intermediate mean decay lengths of the Higgs boson the topology consists of two tracks coming from the interaction point, and with either secondary vertices or kinked tracks. If the Higgs boson decays outside the tracking devices the signature corresponds to stable heavy massive particles. These two analyses were designed for the search for supersymmetric particles decaying to similar topologies. Details can be found in [12].

3.1 Small impact parameter search

An initial set of cuts was applied to select events with four jets of low multiplicity. Only tracks with an impact parameter below 4 cm both in the plane transverse to the beam pipe and in the direction along the beam pipe were considered in the analysis. A charged particle multiplicity between 4 and 8 was required. Events were clustered into jets using the LUCLUS algorithm [6], requiring each jet to be separated from the others by at least 15 degrees, and only events with four reconstructed jets were accepted. To improve the reconstruction of the τ energy, the τ momenta were rescaled, imposing energy and momentum conservation and keeping the τ directions at their measured values. If the rescaled momentum of any jet was negative, the event was rejected, as such events are commonly not genuine four jet events.

The two photon background was reduced by the following energy and momentum requirements: the energy of observed particles produced at a half opening angle to the beam axis exceeding 25° had to be greater than $0.15\sqrt{s}$, the momenta of the jets were required to be larger than $0.01\sqrt{s}$ and the total neutral energy had to be less than $0.35\sqrt{s}$.

The four lepton background was rejected by requiring that the momentum of the most energetic lepton identified (electron or muon) was less than $0.25\sqrt{s}$ and the momentum of the second most energetic lepton identified was less than $0.15\sqrt{s}$. The algorithms used in the lepton identification were the same as those used in the selection of fully-leptonic W pairs [13].

The calculated τ momenta, defined above, were used to reconstruct the Higgs boson mass. The charge of the τ jet was calculated as the sum of the charges of its constituent particles. If this value was not ± 1 , then the charge of the most energetic charged particle was assumed to be the charge of the τ . For events with two positive τ lepton candidates and two negative τ lepton candidates the charge was used to assign the pairing of both doubly charged Higgs bosons. If the total charge was not equal to 0, the pairing was chosen to minimise the difference between the two reconstructed masses of the Higgs bosons. The

ratio $\frac{|M_{H^{++}} - M_{H^{--}}|}{(M_{H^{++}} + M_{H^{--}})/2}$ was required to be less than 0.7. Finally the reconstructed event mass, defined as the average of the two masses, had to be greater than 40 GeV/ c^2 .

The effects of the selection cuts are shown in Table 1 for the combined 189-208 GeV sample. After all cuts were applied only one event was observed in the data with a mass of 69 ± 3 GeV/ c^2 , while 0.9 events were expected from background processes. The candidate was collected at $\sqrt{s}=206.7$ GeV and is compatible with the assignment $ZZ \rightarrow \tau^+ \tau^- \tau^+ \tau^-$. The most probable reconstructed masses with different sign leptons are indeed compatible with a M_Z - M_Z mass hypothesis at the one sigma level. The signal efficiency was around 40% for a wide range of masses between 70 and 100 GeV/ c^2 for both left-handed and right-handed doubly charged Higgs bosons, as shown in Table 2. Table 3 shows the selection efficiencies for left-handed doubly charged Higgs bosons for several $H^{\pm\pm}$ masses and several $h_{\tau\tau}$ couplings at $\sqrt{s}=206.7$ GeV. The final reconstructed mass spectrum and the expected mass distribution in simulated signal events are shown in Figure 1. The good level of agreement between data and simulation observed at different stages of the analysis is demonstrated in Figure 2.

| cut | data | total bkg. | $llll$ | other | $\varepsilon_{H_L^{++}H_L^{--}}$ |
|--------------------------|------|------------------|------------------|------------------|----------------------------------|
| Four jets preselection | 59 | 67.41 ± 0.95 | 44.01 ± 0.31 | 23.40 ± 0.90 | 59.2% |
| anti $\gamma\gamma$ cuts | 26 | 31.03 ± 0.48 | 28.90 ± 0.25 | 2.13 ± 0.41 | 52.3% |
| anti 4 lepton cuts | 1 | 1.87 ± 0.07 | 1.69 ± 0.06 | 0.18 ± 0.03 | 48.7% |
| Mass requirements | 1 | 0.91 ± 0.04 | 0.85 ± 0.04 | 0.06 ± 0.01 | 44.2% |

Table 1: The total number of events observed and the expected background after the different cuts used in the analysis for the small impact parameter search for the combined 189-208 GeV sample. The errors are only statistical. The last column shows the efficiency for a left-handed doubly charged Higgs boson signal with $m_{H_L^{\pm\pm}} = 100$ GeV/ c^2 at $\sqrt{s}=206.7$ GeV. The statistical error in the signal efficiency is about 1.5% in all cases.

| channel | $M_{H^{\pm\pm}}$ (GeV/ c^2) | | | | | |
|--------------|--------------------------------|------|------|------|------|------|
| | 50 | 60 | 70 | 80 | 90 | 100 |
| left-handed | 32.7 | 36.6 | 40.5 | 44.8 | 43.4 | 44.2 |
| right-handed | 31.8 | 37.0 | 40.0 | 44.0 | 44.8 | 45.2 |

Table 2: Selection efficiencies (in %) for left-handed and right-handed $H^{++}H^{--} \rightarrow \tau^+ \tau^+ \tau^- \tau^-$ for several $H^{\pm\pm}$ masses and $h_{\tau\tau} \geq 10^{-7}$ at $\sqrt{s}=206.7$ GeV, for the small impact parameter search. The statistical error is around 1.5% in all cases.

3.1.1 Systematic uncertainties

Several sources of systematic uncertainties on the signal efficiency and the background level were investigated. The particle identification was checked on di-lepton samples both at the Z peak and at high energy. The discrepancy in the efficiencies between the data and the simulation was found to be lower than 2% in all cases. The track selection and the track reconstruction efficiency was also studied with these samples. These effects were studied by the comparison between data and simulation for tracks at the boundaries

| $h_{\tau\tau}$ | $M_{H^{\pm\pm}} \text{ (GeV}/c^2\text{)}$ | | | |
|-------------------|-------------------------------------------|---------------|---------------|--------------|
| | 50 | 70 | 90 | 100 |
| $4 \cdot 10^{-8}$ | 0.2/38.1/13.1 | 1.6/43.0/1.4 | 6.0/23.9/0.0 | 20.5/5.3/0.0 |
| 10^{-8} | 0.0/6.4/68.4 | 0.0/16.0/57.2 | 0.0/30.5/22.7 | 0.0/36.3/7.3 |
| $\leq 10^{-9}$ | 0.0/0.0/77.6 | 0.0/0.0/77.6 | 0.0/0.0/41.3 | 0.0/0.0/41.6 |

Table 3: Selection efficiencies (in %) for left-handed doubly charged Higgs bosons for several $H^{\pm\pm}$ masses and several $h_{\tau\tau}$ couplings at $\sqrt{s}=206.7$ GeV, for the three analyses performed (small impact parameter search, search for secondary vertices or kinks and search for stable massive particles, respectively). The statistical error is around 1.5% in all cases.

of subdetector acceptances, where systematic effects are expected to be larger. The systematic error of these effects was about 1.5%.

The errors on the background and signal rates from the modelling of the detector response were a few percent. Different variables at preselection level have been studied, with good agreement between data and simulation observed. The distributions in relevant variables before the anti $\gamma\gamma$ cuts and the anti four lepton cuts are shown in Figure 2. The masses reconstructed from both same sign and different sign lepton pairs, before the anti four lepton cuts were applied, are shown in Figure 3. For the opposite sign lepton pairs only the mass of the combination closest to the Z mass has been given and the Z peak is clearly visible.

The total systematic error on the background was about 13%, with a dominant contribution of about 12% due to the limited simulation statistics available. The total systematic error on the efficiency was about 5%.

3.2 Search for secondary vertices or kinks

When the lifetime is such that the particle decays inside the tracking detector, the previous analysis is inefficient, because impact parameter cuts are applied to reject the background coming from secondary interactions. We have applied here the analysis described in [12], that performs a special track reconstruction for this particular topology, looking for decay vertices far from the interaction point.

After all cuts five events were selected in the data, while 2.9 events were expected from the background. The signal efficiency was about 40%, if the mean decay length was about 50 cm with a smooth fall for both lower and higher mean decay lengths. The selection efficiencies for several $H^{\pm\pm}$ masses and several $h_{\tau\tau}$ couplings at $\sqrt{s}=206.7$ GeV are shown in Table 3.

3.3 Search for stable massive particles

If the lifetime is even larger, the $H^{\pm\pm}$ crosses the tracking devices without decaying. The analysis described in [12] to search for stable heavy particles is applied here. It is based on the measurement of anomalous ionisation loss measured in the Time Projection Chamber and of the absence of Cherenkov light detected in the Ring Imaging Cherenkov Detector.

One event was selected in the data, in agreement with the expected background of 1.9 events. For stable particle masses in the range of 50-80 GeV/ c^2 the efficiency was $\sim 75\%$, decreasing to $\sim 40\%$ for masses near the kinematic limit (Table 3).

4 Determination of the mass limit

No evidence for $H^{++}H^{--}$ production was observed. A likelihood ratio technique [14] has been used to compute the cross-section and mass limits. The reconstructed event mass was used as a discriminant variable in the computation of the confidence levels in the small impact parameter analysis, while for the others only the number of events were used. The systematic errors were taken into account in the computation. All centre-of-mass energies and the three analyses were treated as independent experiments. For intermediate mean decay lengths of the Higgs bosons in many cases two analyses have significant efficiency. However the overlap of the samples selected by the analyses, both for the signal and for the background, was negligible.

A very similar behaviour, both in terms of efficiency and of mass distributions, was observed for the left-handed and the right-handed doubly charged Higgs bosons. Hence, the average of both contributions were used to calculate the confidence levels. The expected left-handed and right-handed cross-sections were calculated using the PYTHIA generator [6].

Previous searches for $H^{\pm\pm}$ pair production have already excluded $M_{H^{\pm\pm}} < 45.6$ GeV/ c^2 [3]. Therefore, this search was limited to masses greater than this value. The limits at 95% confidence level for different values of $h_{\tau\tau}$ are shown in table 4. Figure 4 shows the 95% confidence level upper limits on the cross-section at $\sqrt{s} = 206.7$ GeV for the production of $H^{++}H^{--} \rightarrow \tau^+\tau^+\tau^-\tau^-$ for these values of $h_{\tau\tau}$. The comparison of these limits with the expected cross-section for left-handed $H_L^{\pm\pm}$ and right-handed $H_R^{\pm\pm}$ pair production yields 95% confidence level lower limits on the mass of the $H_L^{\pm\pm}$ and $H_R^{\pm\pm}$ bosons of 98.1 and 97.3 GeV/ c^2 , respectively for any value of the $h_{\tau\tau}$ coupling.

This search slightly improves previous searches for $h_{\tau\tau} \geq 10^{-7}$ [15], and in addition is extended to the whole range of the $h_{\tau\tau}$ coupling.

| $h_{\tau\tau}$ | Left-handed | | Right-handed | |
|-------------------|-------------|----------|--------------|----------|
| | Observed | Expected | Observed | Expected |
| $\geq 10^{-7}$ | 99.6 | 99.6 | 99.1 | 99.1 |
| $4 \cdot 10^{-8}$ | 98.1 | 98.4 | 97.3 | 97.6 |
| 10^{-8} | 99.0 | 99.4 | 98.4 | 98.9 |
| $\leq 10^{-9}$ | 99.6 | 99.6 | 99.3 | 99.3 |

Table 4: Median expected and observed $H^{\pm\pm}$ mass limits at 95% C.L. in GeV/ c^2 for different values of the $h_{\tau\tau}$ coupling.

5 Conclusion

A search for pair-produced doubly charged Higgs bosons decaying into τ leptons was performed using the data collected by DELPHI at LEP at centre-of-mass energies from 189 GeV to 208 GeV in R-parity conserving supersymmetric left-right symmetric models.

Three different analyses were applied to cover the whole range of the $h_{\tau\tau}$ coupling: decays very close to the interaction point, inside the tracking detectors or beyond them. No significant excess was observed and a lower limit on the doubly charged Higgs boson mass of 97.3 GeV/ c^2 has been set at 95% confidence level for any value of the $h_{\tau\tau}$ coupling. The limits at 95% confidence level for different values of $h_{\tau\tau}$ are summarized in table 4. Figure 4 shows the 95% confidence level upper limits on the cross-section for the process $H^{++}H^{--} \rightarrow \tau^+\tau^+\tau^-\tau^-$ at $\sqrt{s}=206.7$ GeV for these values of the $h_{\tau\tau}$ coupling.

Acknowledgements

We are greatly indebted to our technical collaborators, to the members of the CERN-SL Division for the excellent performance of the LEP collider, and to the funding agencies for their support in building and operating the DELPHI detector.

We acknowledge in particular the support of

Austrian Federal Ministry of Education, Science and Culture, GZ 616.364/2-III/2a/98,
 FNRS-FWO, Flanders Institute to encourage scientific and technological research in the industry (IWT), Belgium,
 FINEP, CNPq, CAPES, FUJB and FAPERJ, Brazil,
 Czech Ministry of Industry and Trade, GA CR 202/99/1362,
 Commission of the European Communities (DG XII),
 Direction des Sciences de la Matière, CEA, France,
 Bundesministerium für Bildung, Wissenschaft, Forschung und Technologie, Germany,
 General Secretariat for Research and Technology, Greece,
 National Science Foundation (NSF) and Foundation for Research on Matter (FOM),
 The Netherlands,
 Norwegian Research Council,
 State Committee for Scientific Research, Poland, SPUB-M/CERN/PO3/DZ296/2000,
 SPUB-M/CERN/PO3/DZ297/2000, 2P03B 104 19 and 2P03B 69 23(2002-2004)
 JNICT-Junta Nacional de Investigação Científica e Tecnológica, Portugal,
 Vedecká grantová agentúra MS SR, Slovakia, Nr. 95/5195/134,
 Ministry of Science and Technology of the Republic of Slovenia,
 CICYT, Spain, AEN99-0950 and AEN99-0761,
 The Swedish Natural Science Research Council,
 Particle Physics and Astronomy Research Council, UK,
 Department of Energy, USA, DE-FG02-01ER41155.

References

- [1] J.F. Gunion, H.E. Haber, G.L. Kane and D. Dawson, The Higgs Hunter's Guide, Frontiers in Physics, Lecture Notes Series, Addison Wesley, 1990;
 C. S. Aulakh, A. Melfo and G. Senjanovic, Phys. Rev. **D57** (1998) 4174;
 Z. Chacko and R. N. Mohapatra, Phys. Rev. **D58** (1998) 15003.
- [2] M. L. Swartz, Phys. Rev. **D40** (1989) 1521;
 K. Huitu et al., Nucl. Phys., **B487** (1997) 27.
- [3] OPAL Collaboration, P. D. Acton et al., Phys. Lett. **B295** (1992) 347.
- [4] DELPHI Collaboration, P. Aarnio *et al.*, Nucl. Instr. and Meth. **A 303** (1991) 233.
- [5] DELPHI Collaboration, P. Abreu *et al.*, Nucl. Instr. and Meth. **A 378** (1996) 57.

- [6] T. Sjöstrand, *PYTHIA 5.719 / JETSET 7.4*, Physics at LEP2, eds. G. Altarelli, T. Sjöstrand and F. Zwirner, CERN 96-01 (1996) Vol 2, 41.
- [7] E. Accomando and A. Ballestrero Comput.Phys.Comm. **99** (1997) 270;
E. Accomando, A. Ballestrero and E. Maina hep-ph/0204052 (2002), to appear in Comput. Phys. Commun.
- [8] F.A. Berends, P.H. Daverveldt, R. Kleiss, Comp. Phys. Comm. **40** (1986) 271, 285 and 309.
- [9] S. Jadach, B.F.L. Ward, Z. Was, Phys. Lett. **B449** (1999) 97;
S. Jadach, B.F.L. Ward, Z. Was, Comp. Phys. Comm. **130** (2000) 260.
- [10] S. Jadach, B.F.L. Ward, Z. Was, Phys. Lett. **390** (1997) 298.
- [11] S. Jadach, W. Placzek, B.F.L. Ward, Comp. Phys. Comm. **79** (1994) 503.
- [12] DELPHI Collaboration, J. Abdallah *et al.*, Search for supersymmetric particles in light gravitino scenarios, to be submitted to Eur. Phys. C.
- [13] DELPHI Collaboration, P. Abreu *et al.*, Phys. Lett. **B479** (2000) 89.
- [14] A.L. Read, in CERN Yellow Report 2000-005, p. 81.
- [15] OPAL Collaboration, G. Abbiendi *et al.*, Phys. Lett. **B526** (2002) 221-232.

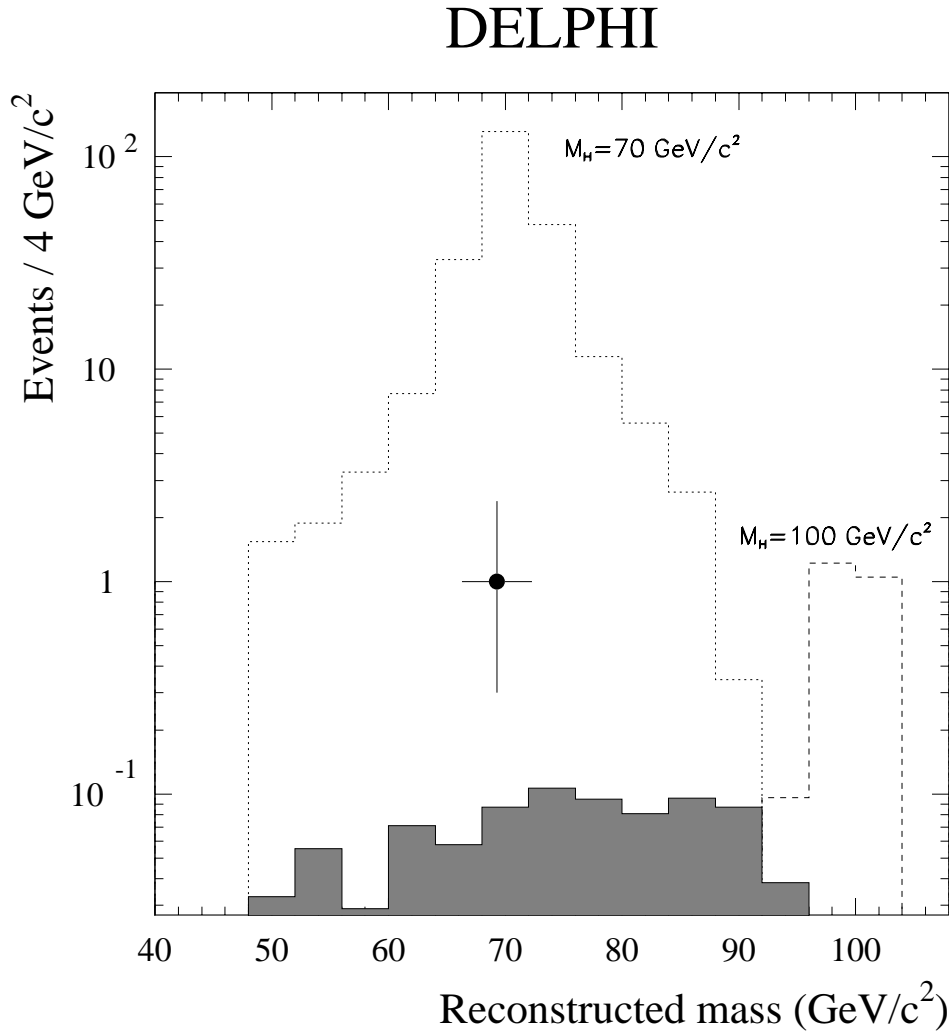


Figure 1: The reconstructed mass distribution after all cuts for the small impact parameter search. The hatched histogram corresponds to the expected background and the dot with the error bar shows the one remaining candidate event. The dotted line corresponds to simulated events with $m_{H_L^{\pm\pm}} = 70 \text{ GeV}/c^2$ and the dashed line corresponds to simulated events with $m_{H_L^{\pm\pm}} = 100 \text{ GeV}/c^2$.

DELPHI

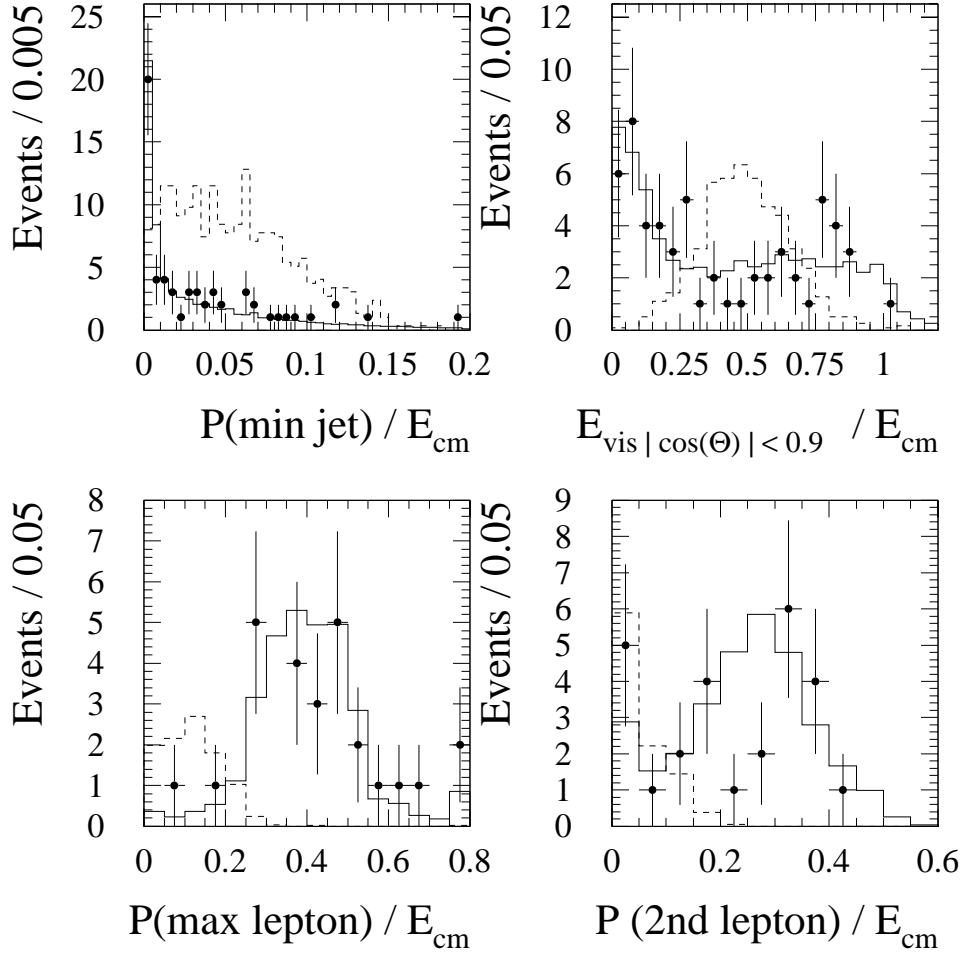


Figure 2: Event selection variable distributions at different stages of the analysis for the small impact parameter search. The top plots show the minimum momentum of the jets and the visible energy outside 25° around the beam pipe scaled by \sqrt{s} after the four jet preselection cuts. The bottom plots show the momentum of the most energetic identified lepton and the momentum of the second most energetic identified lepton scaled by \sqrt{s} after the anti $\gamma\gamma$ cuts. The solid lines show the expected background, the dots the observed data and the dashed lines correspond to $m_{H_L^{\pm\pm}} = 100 \text{ GeV}/c^2$ with arbitrary normalisation.

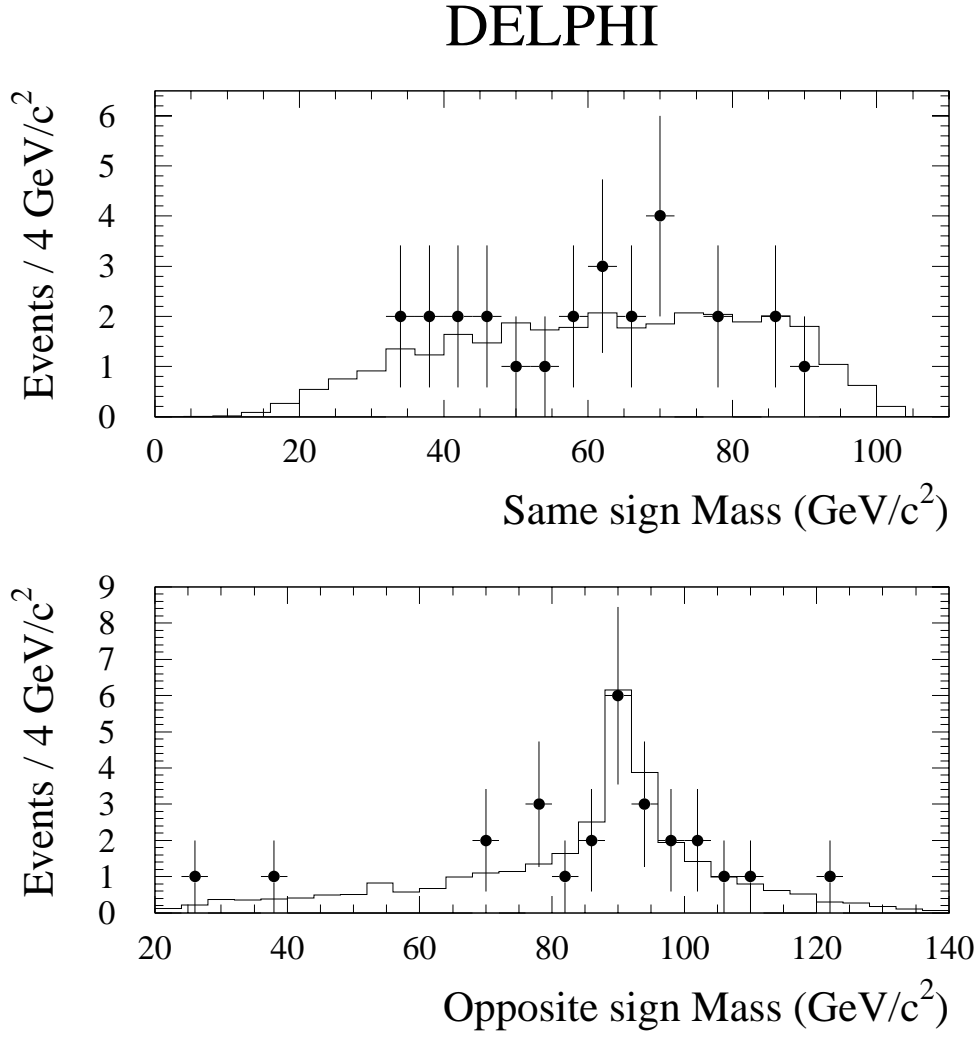


Figure 3: Reconstructed mass distributions for the small impact parameter search. The masses are shown for the same sign lepton pairs (top) and the opposite sign lepton combination closest to the Z mass (bottom). These distributions are shown before the anti four lepton cuts. The solid lines show the expected background and the dots the observed data.

DELPHI

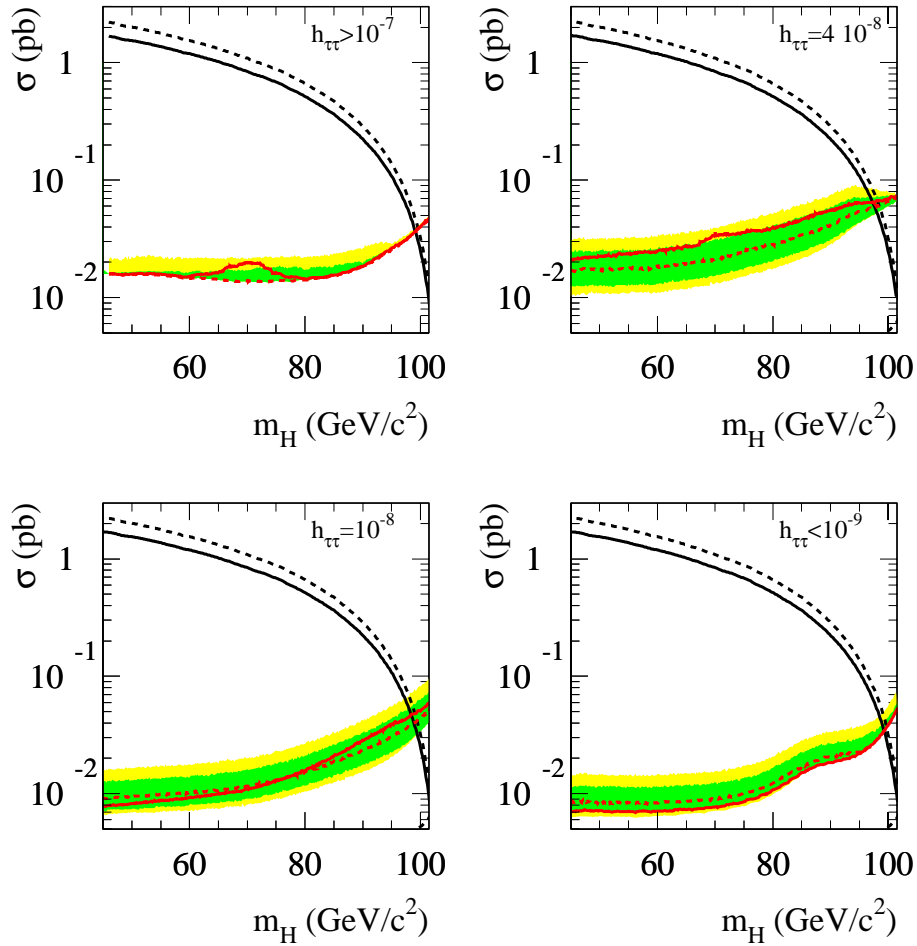


Figure 4: Upper limits, at 95% confidence level, on the production cross-section for a pair of doubly charged Higgs bosons as a function of the doubly charged Higgs boson mass at $\sqrt{s}=206.7$ GeV, assuming 100% branching ratio for the decay of $H^{\pm\pm}$ into $\tau^{\pm}\tau^{\pm}$ for different values of the $h_{\tau\tau}$ coupling. The dashed grey curve shows the expected upper limit with one and two standard deviation bands and the solid grey curve is the observed upper limit of the cross-section (the grey curves are those inside the bands). The dashed black and solid black curves show the expected production cross-section of $H_L^{\pm\pm}$ and $H_R^{\pm\pm}$ pairs in left-right symmetric models.